Systematic growth of $BaFe_{2-x}Ni_xAs_2$ large crystals

2011 Supercond. Sci. Technol. 24 065004

(http://iopscience.iop.org/0953-2048/24/6/065004)

Supercond. Sci. Technol. **24** (2011) 065004 (4pp) doi:10.1088/0953-2048/24/6/065004

Systematic growth of $BaFe_{2-x}Ni_xAs_2$ large crystals

Yanchao Chen[1,2], Xingye Lu[1], Meng Wang[1], Huiqian Luo[1,3] and Shiliang Li[1]

[1] Institute of Physics and National Laboratory for Condensed Matter Physics, Chinese Academy of Sciences, Beijing 100190, People's Republic of China
[2] Science and Technology on Nuclear Date Laboratory, China Institute of Atomic Energy, Beijing 102413, People's Republic of China

E-mail: hqluo@aphy.iphy.ac.cn and slli@aphy.iphy.ac.cn

Received 17 December 2010, in final form 20 February 2011
Published 29 March 2011
Online at stacks.iop.org/SUST/24/065004

Abstract
We have successfully grown large single crystals of $BaFe_{2-x}Ni_xAs_2$ with a series of Ni doping levels from $x = 0$ to $x = 0.30$ by the self-flux method. The resistivity and AC susceptibility measurements show that the superconductivity (SC) smoothly emerges at $x \approx 0.05$, while the antiferromagnetism (AFM) survives up to $x \approx 0.092$. We provide a detailed phase diagram of the $BaFe_{2-x}Ni_xAs_2$ system and suggest that a quantum critical point (QCP) may be located at $x = 0.096 \pm 0.04$.

(Some figures in this article are in colour only in the electronic version)

1. Introduction

The discovery of the Fe-based superconductors [1–4] allows us to investigate another system of high-T_C superconductors besides the cuprates for the first time. Interestingly, the Fe-based superconductors show similar phase diagrams upon doping as those of cuprates where superconductivity emerges from the suppression of long-range AFM order [5–12]. It is thus expected that some of the key features in cuprates should also be found in Fe-based superconductors. The concept of QCP is one of those that are fundamentally important to fully understand the properties of the ground states and finite-temperature excitations in cuprates. In the electron-doped cuprates, the measurements of spin excitations around the area where the AFM order and superconductivity coexist have suggested that a QCP may be located where the AFM order is suppressed to zero by either oxygen annealing or Ce doping [13–15]. The striking similarity between the phase diagrams of electron-doped cuprates and those of the Fe-based superconductors suggests that such a QCP may also be found in the latter. Indeed, it has been shown that a magnetic QCP could result from P doping in $CeFeAs_{1-x}P_xO$ [16, 17].

Here we are interested in the $BaFe_{2-x}Ni_xAs_2$ system, for which high-quality large single crystals are available for various measurements. At room temperature, it has a tetragonal $ThCr_2Si_2$-type structure. The parent compound $BaFe_2As_2$ undergoes a structural transition around 140 K (T_S) [18], resulting in a change of lattice symmetry from tetragonal (I_{4mm}) to orthorhombic (F_{mmm}) space group [19]. In the meantime, the system establishes a three-dimensional long-range AFM order at the same temperature (T_N). Upon doping, both the structural and AFM transitions are suppressed and finally disappear around $x = 0.1$ [10, 11]. Since the ground state changes from long-range AFM to superconductivity, it is possible that a QCP exists in this system as in the electron-doped cuprates [13–15]. From the perspective of crystal growth, it is thus important to provide large single crystals with doping levels around the possible QCP with more details [10, 11].

In this paper, we have systematically grown large single crystals of $BaFe_{2-x}Ni_xAs_2$ with various Ni doping levels, especially around the possible QCP. The whole phase diagram with information on T_S, T_N and superconducting transition T_C is obtained by the resistivity and susceptibility measurement. The doping level of the possible QCP is determined to be $x = 0.096 \pm 0.04$.

2. Experiment

The self-flux method was used to grow $BaFe_{2-x}Ni_xAs_2$ single crystals with the Fe/Ni–As powder as precursor. The Fe, Ni

[3] Author to whom any correspondence should be addressed.

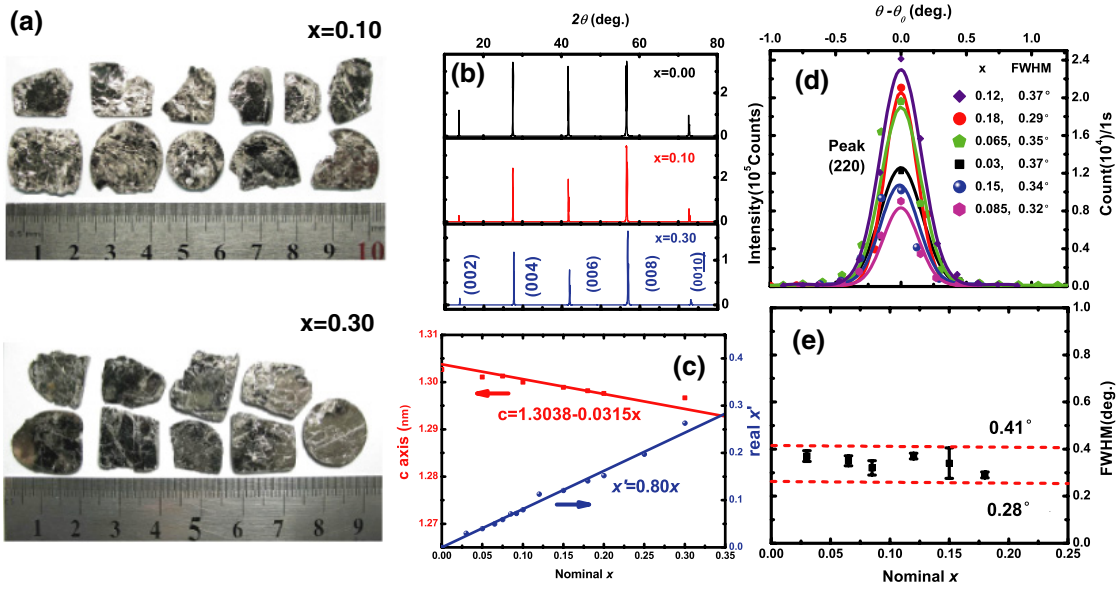

Figure 1. (a) Photos of our samples with nominal Ni doping level $x = 0.10$ and 0.30. The scale unit is centimeters. (b) The x-ray diffraction patterns of $BaFe_{2-x}Ni_xAs_2$ ($x = 0$, 0.10 and 0.30) single crystals at room temperature. (c) Linear relationship between the real Ni concentration x' and the nominal Ni concentration x. The blue line is a straight line, $x' = 0.80x$. Figure 1(c) also shows doping dependence of the lattice constant c deduced from XRD results. The red line is a straight line $c = 1.3038 - 0.0315x$, drawn as a guide for the eyes. (d) Neutron rocking curves of Bragg peak (220) for our samples with nominal Ni doping level $x = 0.03$, 0.065, 0.085, 0.12, 0.15 and 0.18, where θ_0 is the central position of the peak. (e) The summary of peak width, namely full width at half-maximum (FWHM), on each Ni concentration x. The FWHM of our samples is between 0.41° and 0.28° and no satellite peaks are found in our measurements, which indicates the high quality and single domain for each crystal.

powder and ground As chips with a ratio of $2-x$:x:2 are sealed into an evacuated quartz tube. After heating to 500 °C in 10 h and held for more than 20 h, the tube is heated to 700 °C at a rate of 40 °C h^{-1}, holding for 15 h, and then quenched to room temperature. In order to make the precursor homogeneous, the process is repeated three times with the final sintering temperature raised by 20 °C each time. The precursor is mixed with the Ba pieces in the ratio of Ba:$Fe_{1-x/2}Ni_{x/2}As$ = 1:5, where the extra Fe/Ni–As is used as the flux. The mixture is loaded into an aluminum oxide crucible that is sealed in an evacuated quartz tube. The quartz tube is heated up to 900 °C in a muffle furnace and held for more than 10 h to completely melt the barium. For the actual growth of the single crystal, the sample is heated to 1180 °C in 12 h, holding for 10 h, then cooled down to 1050 °C at a rate of 5 °C h^{-1} and finally quenched to room temperature.

X-ray diffraction (XRD) measurements were carried out on a Mac-Science MXP18A-HF equipment at room temperature. The crystalline quality also is examined by a neutron scattering experiment on the E3 spectrometer at the NRU reactor, Chalk River Laboratories in Canada. To check the real doping level of Ni, we have performed the inductively coupled plasma (ICP) analysis. The resistivity and AC magnetization were measured on the physical property measurement system (PPMS, Quantum Design) and the Maglab system (Oxford), respectively. The Néel temperature T_N is also determined by an elastic neutron scattering experiment on the BT-7 spectrometer at the National Institute of Standards and Technology (NIST) in USA.

3. Result and discussion

Figure 1(a) shows the shiny crystals of $x = 0.1$ and 0.3 $BaFe_{2-x}Ni_xAs_2$ samples with the largest size and weight of more than 15 × 15 × 1.5 mm^3 and 1.5 g, respectively. The crystals with other doping levels have similar sizes. We grew more than 20 g crystals for each set of doping levels to meet our demand for the inelastic neutron experiments [20]. The XRD results suggest the high c-axis orientation and crystalline quality of our samples, as illustrated by the examples of $x = 0$, 0.1 and 0.3 samples in figure 1(b). Our previous neutron scattering experiments show that all the measured samples are single domain [20]. Figures 1(d) and (e) also give the neutron rocking curves of our crystals with nominal Ni doping level $x = 0.03$, 0.065, 0.085, 0.12, 0.15 and 0.18. The peak width FWHM of (220) is always between 0.41° and 0.28°, which indicates the high quality of our samples.

The composition of our samples are determined by the ICP analysis method. Assuming the ratio of Fe:Ni is $(2 - x')$:x', we found that the real Ni doping level x' is smaller than the nominal Ni doping level x. In fact, there is a linear relationship between x' and x with $x' = 0.8x$, as shown in figure 1(c), suggesting a segregation coefficient $K = C_s/C_l$ of about 0.80 during the crystallization. Such a coefficient is consistent with other reports [11], indicating some kind of intrinsic crystal growth process in this system. In this paper, we will only use the nominal concentration x in the following discussion. The lattice parameter has a similar linear dependence on Ni doping. Figure 1(c) shows the c-axis constant deduced from XRD results, changing from 1.303 nm in the parent compound

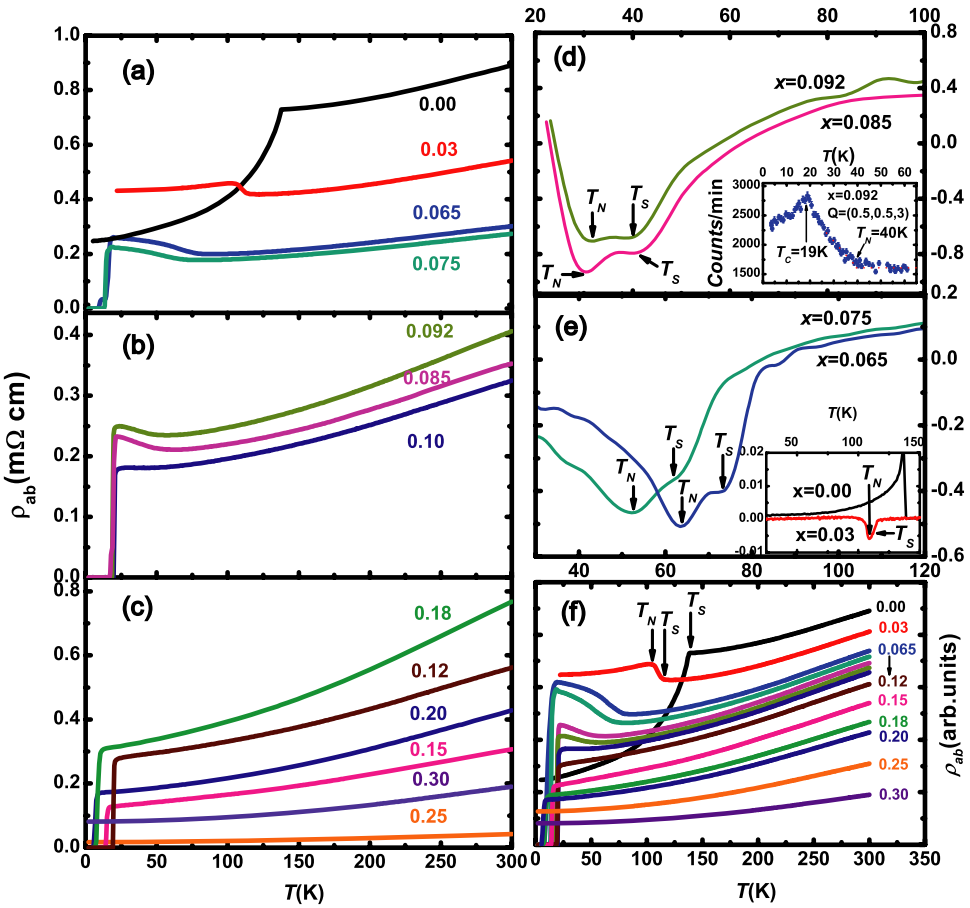

Figure 2. The temperature dependence of resistivity in the ab plane and the first-order derivative of temperature, where T_N and T_S are indicated by arrows. (a)–(c) In-plane resistivity $\rho_{ab}(T)$ for each doping concentration x. (d) The first-order derivative of the resistivity for $x = 0.085$ and 0.092 (main panel) and the temperature dependence of the intensity of the magnetic Bragg peak (0.5, 0.5, 3) measured by elastic neutron experiment (insert) which confirms the Néel temperature $T_N = 40$ K. (e) The first-order derivative of the resistivity for $x = 0$ and 0.30 (inset) and $x = 0.065$ and 0.075 (main panel). (f) Normalized in-plane resistivity $\rho_{ab}(T)$ by assuming a linear doping dependence of the resistivity at room temperature ρ_{ab} (300 K).

to 1.297 nm in the $x = 0.3$ compound. The variation of lattice parameter is much smaller than in a hole-doped compound like $Ba_{1-x}K_xFe_2As_2$ [21], because the substitution of Fe by Ni happens in the Fe–As plane in the electron-doped compound, while in the hole-doped compound it is out-of-plane substitution of Ba by K.

Figures 2(a)–(c) show the temperature dependence of in-plane resistivity $\rho_{ab}(T)$ for each doping level. In order to get the evolution of the curvature of $\rho_{ab}(T)$, we simply normalize the data by assuming a linear doping dependence of the resistivity at room temperature ρ_{ab} (300 K). The results are shown in figure 2(f). Upon doping, the lineshape of $\rho_{ab}(T)$ has a systematic evolution and the abnormal 'kinks' are gradually suppressed, too. The kink at about 134 K in the resistivity of the $x = 0$ sample is associated with the first-order structural and magnetic phase transitions [18, 19, 22]. With Ni doping, these two transitions separate from each other, which results in two kinks in the first derivative of the resistivity [11, 23], as shown in figures 2(d) and (e). Both kinks persist up to a doping level of $x = 0.092$. Neutron scattering experiments have shown that the kinks at higher and lower temperatures represent the structural transition temperature T_S and the AFM transition temperature T_N, respectively. At $x = 0.10$, no kink is found in the normal state of $\rho_{ab}(T)$, which is consistent with the neutron scattering results that neither long-range AFM order nor orthorhombic structure exist at this doping level [24].

The superconducting properties are also checked by the AC magnetic susceptibility measurement. All the data are given in figure 3, where both the real part χ' and the imaginary part χ'' are normalized to their values at 2 K. The transition width is less than 2 K in the whole doping range, suggesting the high quality of superconductivity in our samples.

Considering all the data from the resistivity, magnetic susceptibility and elastic neutron scattering experiments, we obtain the phase diagram as shown in figure 4. It is clear that superconductivity coexists with the long-range AFM order up to $x = 0.092$. We thus conclude that a QCP, if it exists, must be located at $x = 0.096 \pm 0.04$, where the error bar is chosen as half the value of the difference between $x = 0.10$ and 0.092. According to the above relationship between the nominal and real Ni concentration we gave, this amounts to $x' = 0.0768 \pm 0.0032$.

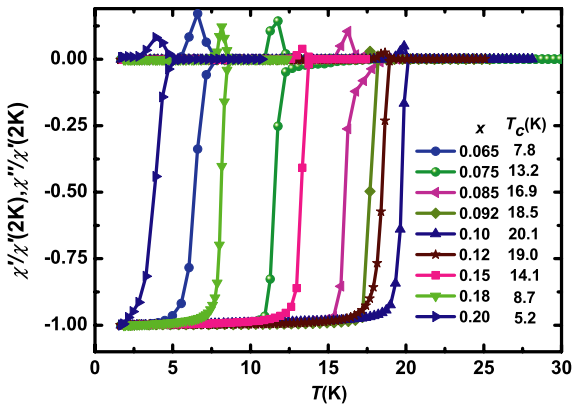

Figure 3. Normalized AC magnetic susceptibility for the samples with x from 0.065 to 0.20. The superconducting transition temperature T_C is defined as the point where the real part deviates from the flattened normal-state susceptibility. All samples show sharp superconducting transitions with widths of about 2 K.

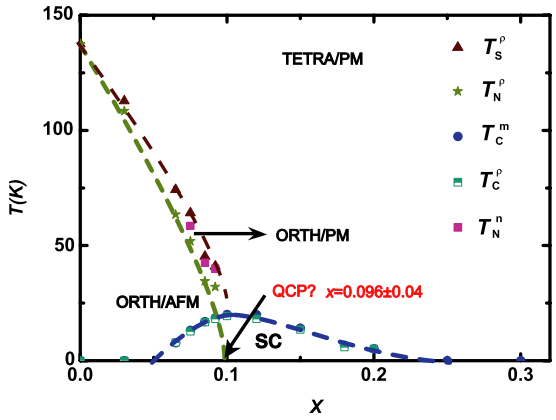

Figure 4. The phase diagram of $BaFe_{2-x}Ni_xAs_2$ for $0.00 \leqslant x \leqslant 0.30$. The T_N^ρ, T_S^ρ and T_C^ρ are the AFM transition temperature, structure transition temperature and superconducting transition temperature derived from resistivity, respectively. T_N^n is the AFM transition temperature obtained from elastic neutron scattering and T_C^m is the superconducting transition temperature obtained from AC susceptibility measurements. All lines are guides for the eyes.

4. Summary

High-quality large single crystals of Ni-doped $BaFe_2As_2$ were grown successfully by the self-flux method. After establishing the phase diagram by the resistivity and AC susceptibility measurements, we conclude that a possible QCP may be located at the nominal doping level $x = 0.096 \pm 0.04$. Our results suggest that any future study on the properties around the QCP regime should concentrate on this doping level.

Acknowledgments

This work was financially supported by the Natural Science Foundation of China, the Ministry of Science and Technology of China (973 Project nos. 2010CB833102, 2010CB923002 and 2011CBA00110), and the Chinese Academy of Sciences. The authors acknowledge the neutron scattering experiments with the help of Miaoyin Wang and Pengcheng Dai at the University of Tennessee, USA, Sung Chung and Jeffery Lynn at the National Institute of Standards and Technology, USA, and Zahra Yamani at the National Research Council, Chalk River Laboratories, Canada.

References

[1] Kamihara Y, Watanabe T, Hirano M and Hosono H 2008 *J. Am. Chem. Soc.* **130** 3296
[2] Chen X H, Wu T, Wu G, Liu R H, Chen H and Fang D F 2008 *Nature* **453** 761
[3] Chen G F *et al* 2008 *Phys. Rev. Lett.* **100** 247002
[4] Ren Z A *et al* 2008 *Europhys. Lett.* **82** 57002
[5] Vaknin D *et al* 1987 *Phys. Rev. Lett.* **58** 2802–5
[6] de la Cruz C *et al* 2008 *Nature* **453** 899
[7] Zhao J *et al* 2008 *Nat. Mater.* **7** 953
[8] Huang Q *et al* 2008 *Phys. Rev.* B **78** 054529
[9] Yeh K *et al* 2008 *Europhys. Lett.* **84** 37002
[10] Li L J *et al* 2009 *New J. Phys.* **11** 025008
[11] Ni N *et al* 2010 *Phys. Rev.* B **82** 024519
[12] Drew A J *et al* 2009 *Nat. Mater.* **8** 310
[13] Wilson S D *et al* 2006 *Phys. Rev.* B **74** 144514
[14] Motoyama E M *et al* 2007 *Nature* **445** 186
[15] Dagan Y *et al* 2004 *Phys. Rev. Lett.* **92** 167001
[16] de la Cruz C *et al* 2010 *Phys. Rev. Lett.* **104** 017204
[17] Luo Y *et al* 2010 *Phys. Rev.* B **81** 134422
[18] Rotter M, Tegel M, Johrendt D, Schellenberg I, Hermes W and Pöttgen R 2008 *Phys. Rev.* B **78** 020503(R)
[19] Rotter M, Tegel M and Johrendt D 2008 *Phys. Rev. Lett.* **101** 107006
[20] Wang M *et al* 2010 *Phys. Rev.* B **81** 174524
[21] Luo H Q, Wang Z S, Yang H, Cheng P, Zhu X Y and Wen H H 2008 *Supercond. Sci. Technol.* **21** 125014
[22] Dong J *et al* 2008 *Europhys. Lett.* **83** 27006
[23] Chu J H *et al* 2009 *Phys. Rev.* B **79** 014506
[24] Chi S X *et al* 2009 *Phys. Rev. Lett.* **102** 107006